Solution Properties of Hyaluronic Acid and Comparison of SEC-MALS-VIS Data with Off-Line Capillary Viscometry

Stepan Podzimek,[1] Martina Hermannova,[2] Helena Bilerova,[2] Zuzana Bezakova,[2] Vladimir Velebny[2]

[1]SYNPO a.s., Department of Analytical and Physical Chemistry, S.K. Neumanna 1316, Pardubice CZ-532 07, Czech Republic
[2]CPN spol. s r.o., Laboratory of Instrumental Analysis, Dolni Dobrouc 401, Dolni Dobrouc CZ-561 02, Czech Republic

ABSTRACT: Extensive study of solution properties of sodium hyaluronate including about 140 samples and covering broad molar mass range was carried out by classical viscometry using an Ubbelohde capillary viscometer and by combination of size-exclusion chromatography with a multi-angle light scattering detector and an on-line viscometer. The study also involved critical overview of literature data of Mark-Houwink relation for sodium hyaluronate. Continuous decrease of the Mark-Houwink exponent with increasing molar mass to the values markedly lower than those typical of linear random coils in thermodynamically good solvents was observed. This fact was attributed to branched molecular structure of hyaluronic acid as a result of unknown side reactions during the manufacturing process. The molar mass dependence of the second virial coefficient was determined and proved aqueous salt solutions to be thermodynamically good solvents for sodium hyaluronate. © 2010 Wiley Periodicals, Inc. J Appl Polym Sci 116: 3013–3020, 2010

Key words: sodium hyaluronate; hyaluronic acid; Viscometry; light scattering; size-exclusion chromatography

INTRODUCTION

Sodium hyaluronate (sodium salt of hyaluronic acid, HA), a naturally occurring polysaccharide chemically classified as a glycosaminoglycan, is composed of alternating β-(1→4) linked *N*-acetyl-D-glucosamine and β-(1→3) linked D-glucuronic acid.[1] HA is found in the synovial joint fluid, the vitreous humor of the eye, the cartilage, blood vessels, extracellular matrix, skin, and the umbilical cord. Many exceptional physicochemical properties of HA, e.g., unique viscoelastic properties and water retention capacity, allow its various applications especially in the pharmaceutical, medical, and cosmetic fields. Ongoing research is now focusing on the use of HA in drug delivery systems, in addition to its present various therapeutic applications in ophtalmology, dermatology, and osteoarthritis.[2] The characterization of HA hydrodynamic properties and detailed knowledge of the molecular structure are very important for efficient applications. Despite intensive studies devoted to the molecular structure of HA and behavior of its dilute solutions, it seems that some experimental data were misinterpreted, and that the molecular structure and explanation of rheological behavior of dilute solutions may be different from commonly accepted ones.

The intrinsic viscosity [η] represents one of the most important variables describing the behavior of a dilute polymer solution. It is a measure of the hydrodynamic volume occupied by a macromolecule in solution and therefore a reflection of its size. The relation between the intrinsic viscosity and molar mass (called Mark-Houwink or Mark-Houwink-Kuhn-Sakurada relation):

$$[\eta] = K \times M^a \tag{1}$$

provides direct information about the configuration and conformation of polymer chains in a dilute solution under given conditions (i.e., solvent and temperature). The Mark-Houwink plots of linear polymers are linear over entire molar mass range while curved plots indicate branched structure. The slope of the plot, i.e., Mark-Houwink exponent *a*, bears information about the polymer-solvent interactions and molecular conformation and configuration. The *a* values for linear polymers in thermodynamically good solvents are around 0.7; the values in the range of about 0.8–1.0 (rarely up to 2) indicate

extended rod-like conformation; in so called theta conditions the exponent *a* equal to 0.5; and for compact spheres the *a* is zero. Note: The coil behavior of linear polymers gradually disappears at low polymerization degrees, but such oligomers were not studied in this article. The Mark-Houwink equation is also often used for the determination of average molar mass. However, the accuracy of the molar masses obtained in this way depends greatly on the reliability of *K* and *a* parameters. The sample must be measured under identical conditions as those used for the determination of Mark-Houwink parameters, and the viscometric method yields incorrect results in case of branched polymers. The Mark-Houwink parameters of HA have been determined previously by several researchers. Most of the studies (with a few exceptions)[3,4] used off-line methods and nonfractionated samples with broad molar mass distribution. Mark-Houwink exponent was reported to depend on molar mass of HA.[3,5–8] The decrease of the exponent *a* with increasing molar mass was explained due to either (i) transition from rod-like conformation at low molar masses to random coil conformation at high molar masses or (ii) decrease of [η] due to shear rate dependent viscosity (non-Newtonian flow behavior). Serious and frequent drawback of previously published results was relatively low number of analyzed samples. For instance, three different Mark-Houwink exponents were reported by Hokputsa et al. based on solely six experimental data points.[5]

In this article, we describe the study of the molar mass dependence of [η] measured by about 140 HA samples, which were characterized by classical procedure using Ubbelohde viscometer and by combination of size-exclusion chromatography (SEC) with a multi-angle light scattering photometer (MALS) and an on-line viscometer (VIS).

EXPERIMENTAL PART

General methods

High-molar-mass HA samples were manufactured by a fermentation process in Contipro Group Holding Companies (Dolni Dobrouc, Czech Republic). To prepare samples with lower molar masses, the aqueous 1% HA solutions (adjusted to pH 5, 4, or 3 with 5% HCl) were heated under reflux in a heating mantle at 100°C for 1 to 240 min. The degraded samples were cooled down to room temperature immediately, and then pH was adjusted with 5% NaOH to 6.5–7.5. Degraded HA was precipitated in the presence of sodium chloride (8 g/L) with isopropanol or ethanol, then dewatered with the respective alcohol and dried at 60°C to a constant weight. The relation between the number-average polymerization degree and hydrolysis time is given by the equation:
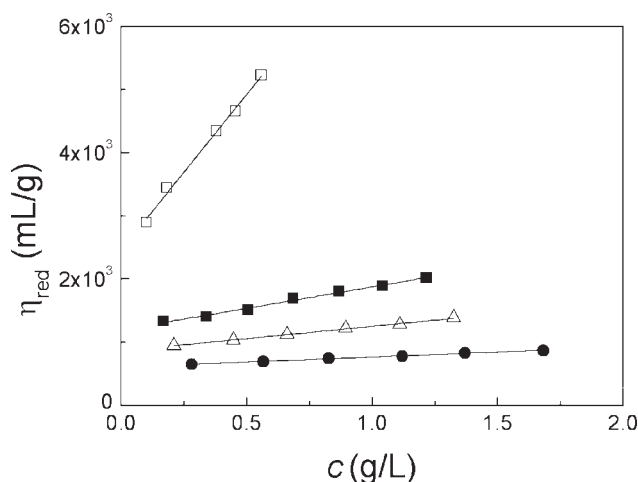
Figure 1 Reduced viscosity versus concentration plots for HA samples of $M_w = 2.6 \times 10^6$ g/mol (□), 7.8×10^5 g/mol (■), 5.5×10^5 g/mol (△), and 3.35×10^5 g/mol (●).

$$1/P_{nt} = k \times t + 1/P_{n0} \qquad (2)$$

where P_{n0} and P_{nt} are the original polymerization degree and the polymerization degree obtained after time *t*, respectively. The constant *k* is 1×10^{-5} s^{-1}, 7×10^{-5} s^{-1}, and 2×10^{-4} s^{-1} for the acidic depolymerization at pH 5, 4, and 3, respectively. The details of HA degradation are reported in reference.[9]

Intrinsic viscosity

The intrinsic viscosities were measured using an Ubbelohde viscometer with the capillary diameter of 0.636 mm. Measurements were performed in aqueous 0.1*M* sodium phosphate buffer pH 7, 1*M* sodium chloride, 1*M* sodium iodide, and 5*M* guanidine hydrochloride at 25°C ± 0.2°C. Each determination was carried out at least three times and the average value was used as the result. The intrinsic viscosity was determined by linear extrapolation of the concentration dependence of reduced viscosity (specific viscosity divided by concentration) to zero concentration.[10] At least five concentrations were used for the [η] determination and to increase the reliability of the measurements each concentration was prepared separately by weighing instead of usual procedure of the dilution of stock solution. The concentration ranges were about 0.05–0.5 mg/mL for samples with molar masses over 2×10^6 g/mol to 2–10 mg/mL for the samples with the lowest molar masses of around 3×10^4 g/mol. All plots of reduced viscosity versus concentration were perfectly linear (see Fig. 1), which indicates that the measurements were performed below the critical overlap concentration. All intrinsic viscosities in this article are expressed in mL/g.

The maximum shear rate $\dot{\gamma}_{max}$ at the wall of the capillary of Ubbelohde viscometer was calculated according to the equation:

$$\dot{\gamma}_{max} = \frac{4V}{\pi R^3 t} \tag{3}$$

where V is the volume that flows through the capillary per unit time t, and R is the radius of the capillary.

SEC-MALS-VIS

The chromatographic system consisted of an Agilent degasser Model G 1379A, an Agilent HPLC pump Model G 1310A, a Rheodyne manual injector Model 7125i, two 300 × 7.8 mm Ultrahydrogel Linear columns (Waters), a DAWN EOS multi-angle light scattering photometer (Wyatt Technology Corporation), a ViscoStar on-line differential viscometer (Wyatt Technology Corporation) and a Waters 410 differential refractive index detector. Injection volume was 100 μL of 0.015 – 1% w/v HA solutions. The mobile phase was aqueous 50 mM sodium sulphate and 0.02% sodium azide at the flow rate of 0.5 mL/min. Data collection and processing were performed using the ASTRA software, Version 5.3.1.4 (Wyatt Technology Corporation). The specific refractive index increment of 0.155 mL/g was used for HA and 0.145 mL/g for dextran and pullulan. Each sample was filtered through Millex-HN Nylon 0.45 μm, 25 mm diameter syringe filter (Millipore). All reagents for SEC were HPLC grade and the mobile phase was filtered through Durapore VVPP 0.1 μm Membrane Filter (Millipore).

Berry light scattering formalism was used for the processing of light scattering data. The obtained plots of logarithm of molar mass versus elution volume were approximately linear with no deviations at the end of chromatograms (for typical example see Fig. 2). No result fitting was used. The sample mass recoveries were close to 100%.

Determination of the specific refractive index increment

Pharmaceutical grade sodium hyaluronate, with the molar mass from 10^4 up to $1.5 × 10^6$ g/mol, was used for dn/dc measurements. The refractive indices of a series of six dilutions of HA in the particular solvent with concentrations between 0.5 and 5 mg/mL for 10^4 g/mol HA sample and 0.1–1 mg/mL for $1.5 × 10^6$ g/mol HA sample were determined at 690 nm using the Optilab rEX refractometer, and the dn/dc was calculated using the ASTRA V software. The mean value of more than 20 dn/dc measurements was $0.155 ± 0.002$ mL/g. Similar procedure was used for the determination of dn/dc of pullulan and
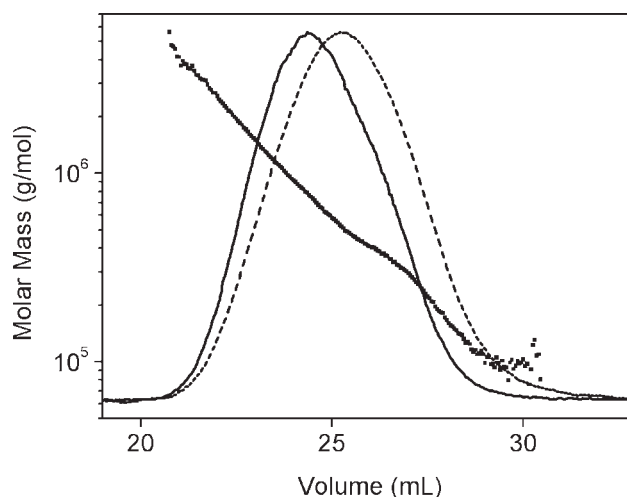

Figure 2 Typical SEC-MALS chromatograms recorded by MALS (full line) and RI (dashed line) detectors, and molar mass versus elution volume plot for HA of $M_w = 7 × 10^5$ g/mol.

dextran using the concentration range of 0.5–5 mg/mL.

Rheological measurements

A TA Instruments AR-G2 rheometer was used to measure the dynamic viscosities of the HA solutions in the range of shear rate 0.001–5000 s^{-1}. Stainless steel double concentric cylinder geometry was used under steady state mode. The sample temperature was maintained at 25°C using a Peltier temperature control system. The data were evaluated by data analysis software, and the dynamic viscosities at low shear rates were extrapolated to zero shear rate using a Cross model. The critical shear rates were determined as a transition between the Newtonian and non-Newtonian (shear-thinning) parts of the flow curves.

Determination of the second virial coefficient

The second virial coefficients (A_2) of HA samples of various molar masses were determined by static light scattering in a batch mode. The measurements were carried out using a DAWN EOS photometer in so-called micro-batch mode. The intensity of scattered light was measured at 16 angles at 5 s intervals. Using a syringe pump the solutions were continuously pumped into the flow cell at a flow rate of about 0.5 mL/min being on-line filtered with 0.45-μm Millex-HN Nylon 25 mm diameter syringe filter. At least six different sample concentrations were used for Zimm plot construction. The specific refractive index increment of 0.155 mL/g was used for HA. Data acquisition and processing were performed using the Wyatt Technology Corporation ASTRA software, Version 5.3.1.4. The concentration
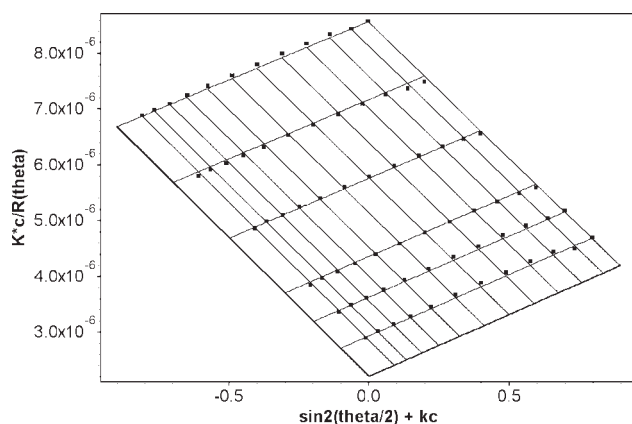
Figure 3 Example of Zimm plot for HA: $M_w = 4.53 \times 10^5$ g/mol, $R_z = 72$ nm, $A_2 = 2.8 \times 10^{-3}$ mol mL g^{-2}.

ranges were 0.3–3 mg/mL for samples with molar masses around 1×10^5 g/mol to 0.02–0.2 mg/mL for samples with the highest molar masses of about 2.2×10^6 g/mol. The first order fit of Zimm model was used for data processing of all samples (for example see Fig. 3).

RESULTS AND DISCUSSION

Figure 4 depicts intrinsic viscosities of HA samples plotted against corresponding weight-average molar masses (M_w). The two series of data points were obtained by Ubbelohde viscometer using the M_w determined by SEC-MALS, and by means of SEC-MALS-VIS. In the latter case the M_w and the weight-average intrinsic viscosities were calculated for the entire peaks. As can be seen in Figure 4 the two Mark-Houwink plots obtained by two different methods are markedly curved in the entire molar mass range. The shift of the plot obtained from SEC-MALS-VIS measurements toward slightly higher intrinsic viscosities can be explained by lower salt concentration and consequently higher polymer coil expansion due to repulsive electrostatic forces. By fitting the data with the second order polynomial and subsequently taking the derivative of that function, one can determine instantaneous a values as a function of molar mass. The following equations and the correlation coefficients were obtained for the data acquired with the Ubbelohde viscometer and SEC-MALS-VIS, respectively:

$$\log[\eta] = -0.118(\log M_w)^2 + 2.077 \log M_w - 5.085,$$
$$r = 0.993 \quad (4)$$

$$\log[\eta] = -0.145(\log M_w)^2 + 2.350 \log M_w - 5.610,$$
$$r = 0.999 \quad (5)$$

The a values range from 1.03 at low molar masses to 0.55 at high molar masses for the Ubbelohde data,
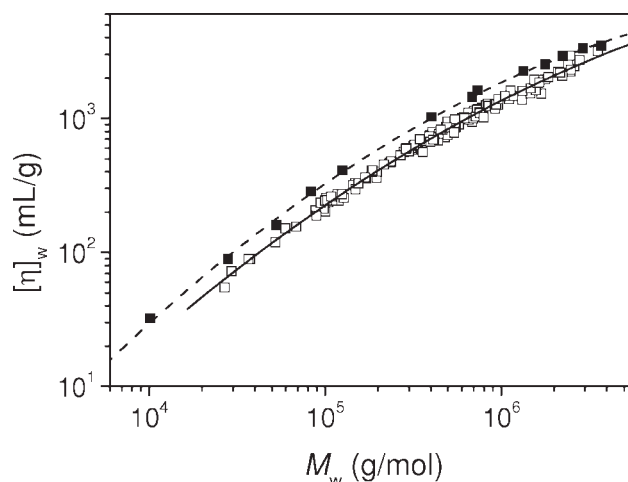
Figure 4 Intrinsic viscosity of sodium hyaluronate plotted as a function of weight-average molar mass according to the Mark-Houwink relationship. Data obtained by Ubbelohde viscometer in 0.1M sodium phosphate buffer pH 7 (□), data from SEC-MALS-VIS measurements in 0.05 M sodium sulphate (■). Mathematical data fits: eqs. (4) and (5). Sample polydispersities ranged from 1.3 (high-molar-mass samples) to 1.8 (lower-molar-mass samples).

and from 1.06 to 0.47 for the SEC-MALS-VIS measurements. The scattering of data points obtained by Ubbelohde viscometer can be explained by different sample properties rather than by experimental uncertainties as each data point was carefully measured at least three times. The scattering of data points vividly illustrates how false conclusions can easily be drawn if low number of experimental data points is used.

Figure 5 presents Mark-Houwink plots of 6 samples obtained in SEC-MALS-VIS mode. The samples were selected to cover similar molar mass range as in Figure 4 and to have overlapping molar mass distributions. In contrast to Figure 4 where the weight-
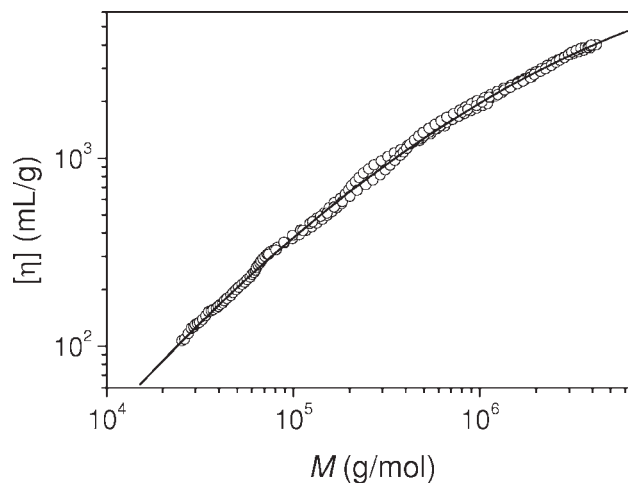

Figure 5 Overlay of Mark-Houwink plots of 6 HA samples of different molar mass distribution measured using SEC-MALS-VIS. Mathematical data fit eq. (6).
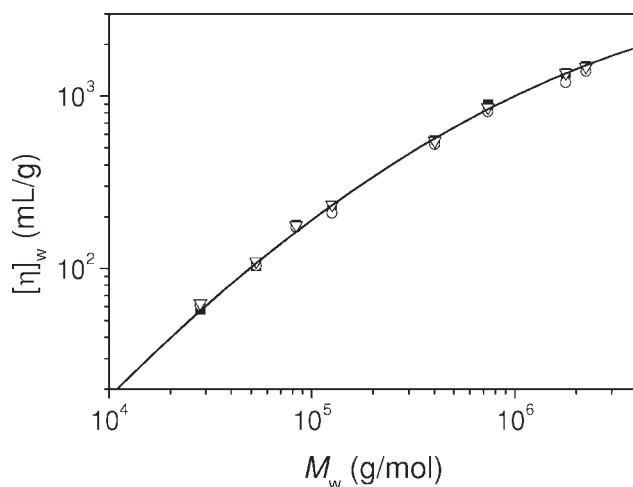
Figure 6 Intrinsic viscosity of sodium hyaluronate plotted as a function of weight-average molar mass according to the Mark-Houwink relationship. Data obtained by Ubbelohde viscometer in 1M sodium chloride (■), 1M sodium iodide (○), and 5M guanidine hydrochloride (▽). Mathematical data fit eqs. (7), (8), and (9).

averages are used, the particular data points are valid for almost monodisperse fractions eluting from SEC columns. The overall plot is markedly curved and can be described by an analogous fit as the plots in Figure 4:

$$\log[\eta] = -0.123(\log M_w)^2 + 2.075 \times \log M - 4.721,$$
$$r = 0.997 \quad (6)$$

The corresponding a values for the lowest ($M = 2.5 \times 10^4$ g/mol) and highest ($M = 3.9 \times 10^6$ g/mol) molar masses are 0.99 and 0.45, respectively. The

log-log relations of the intrinsic viscosity and molar mass determined by the batch and on-line experiments are in good agreement, which corresponds to the previously reported results.[11]

To strongly suppress intermolecular and intramolecular ionic and hydrophobic interactions and hydrogen bonds, the intrinsic viscosities were determined in 1M sodium chloride, 1M sodium iodide, and 5M guanidine hydrochloride (G.HCl). The results depicted in Figure 6 show that at high concentrations the effect of salt type is negligible and all three Mark-Houwink plots almost overlap. The plots are markedly curved and can be described by the following second order polynomial fits:

1M NaCl

$$\log[\eta] = -0.155(\log M_w)^2 + 2.422 \times \log M - 5.953,$$
$$r = 0.998 \quad (7)$$

1M NaI

$$\log[\eta] = -0.137(\log M_w)^2 + 2.208 \times \log M - 5.317,$$
$$r = 0.999 \quad (8)$$

5M G.HCl

$$\log[\eta] = -0.135(\log M_w)^2 + 2.173 \times \log M - 5.223,$$
$$r = 0.998 \quad (9)$$

As against the Figures 4 and 5 the high concentrations of salts result in a shift of the plots toward lower intrinsic viscosities due to more coiled conformation. The slopes of the plots (exponents a) get close to 0.5 for molar masses close to 2×10^6 g/mol.

TABLE I
Mark-Houwink Parameters Reported in Literature for HA

| Range of M (g/mol)	K (mL/g)	a	Solvent	Temperature (°C)	Reference
< 100,000	0.0013	1.056	0.15M NaCl	37	3
100,000–1,000,000	0.0339	0.778			
> 1,000,000	0.3950	0.604			
< 100,000	-	1.000	0.15M PBS pH 7.3	20	5
100,000–1,000,000		0.730			
> 1,000,000		0.690			
< 1,000,000	0.0035	0.779	0.15M NaCl	25	6
> 1,000,000	0.0397	0.601			
10,000–72,000	0.0003	1.200	0.20M PBS pH 7.3	37	7
310,000–1,500,000	0.0570	0.760			
400,000–2,000,000	0.0508	0.716	0.20M NaCl	20	8
	0.0302[a]	0.770[a]			
77,000–1,700,000	0.0360	0.780	0.20M NaCl	25	12
150,000–4,300,000	0.0160	0.841	0.10M NaCl	25	13
700,000–1,500,000	0.0403	0.775	0.20M NaCl	25	14
400,000–2,700,000	0.0199	0.829	0.20M NaCl	25	15
100,000–1,000,000	0.0570	0.750	0.15M NaCl	25	16
100,000– 3,000,000	0.0290	0.800	0.15M NaCl	25	17
420,000–1,400,000	0.0278	0.780	0.10M NaNO$_3$	25	18

[a] Determined by Zimm-Crothers viscometer.
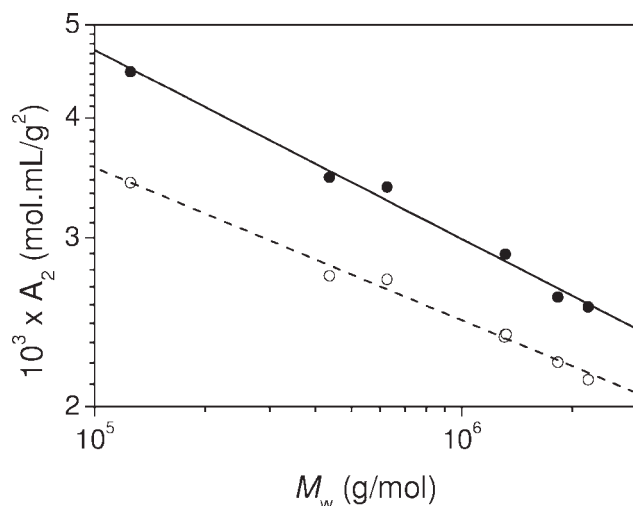
Figure 7 Molar mass dependence of the second virial coefficient of HA determined by static light scattering in 0.1M sodium phosphate buffer ($\bigcirc$) and 0.05M sodium sulphate ($\bullet$). Mathematical data fit eqs. (10) and (11).

It is obvious that the Mark-Houwink plots obtained by numerous measurements of about 140 samples employing different techniques and different aqueous solvents have similar curved shapes, with the exponent a starting at about 1 at molar mass of the order of magnitude of several tens g/mol and evenly decreasing to about 0.5 at molar mass of the order of magnitude of several millions g/mol. The decrease of the Mark-Houwink exponent was published by several authors (see Table I) and explained by the change of chain conformation from rod-like to random coil or by non-Newtonian flow behavior. However, both theories have significant weaknesses as discussed hereafter.

As showed in this work and previously by Waters and Leiske,[4] the exponent a reaches the value close to 0.5. In our work, the a equal to 0.5 is reached for molar mass of about 2×10^6 g/mol, but Waters and Leiske obtained the exponent a close to 0.5 for molar mass as low as 8×10^5 g/mol, which may have simple explanation that they measured different samples. In so called theta conditions the second virial coefficient (A_2) is equal to zero mol mL/g^2 and the Mark-Houwink exponent to 0.5. However, the second virial coefficients obtained by classical light scattering experiments prove the aqueous salt solutions to be thermodynamically good solvents for HA. The following relations between the second virial coefficient and molar mass in 0.1M sodium phosphate buffer [eq. (10)] and 0.05M sodium sulphate [eq. (11)] at 25°C were found:

$$A_2 = 0.022 \times M_w^{-0.159} \text{ mol mL/g}^2, \quad r = 0.989 \quad (10)$$

$$A_2 = 0.045 \times M_w^{-0.197} \text{ mol mL/g}^2, \quad r = 0.991 \quad (11)$$

The corresponding graphical plots of A_2 versus M_w are in Figure 7. The A_2 values are of the order of magnitude of 10^{-3} mol mL/g^2 over all investigated molar masses and in both solvents used for the measurements. The A_2 of 2.5×10^{-3} mol mL/g^2 was previously reported by Ghosh et al.[19] The A_2 values are about an order of magnitude higher than those of various synthetic and natural polymers in thermodynamically good solvents. For example, the A_2 of 3×10^{-4} mol mL/g^2 was determined for dextran of $M_w = 5 \times 10^5$ g/mol in 0.05M sodium sulphate. On the basis of the high A_2, one would expect a around 0.7; and taking into account stiffness of HA chain even higher values would be more probable. It is evident that from the thermodynamic viewpoint the Mark-Houwink exponents for linear HA around 0.5 are highly unlikely.

The decrease of a due to shear rate dependent viscosity was reported to appear at molar masses over 10^6 g/mol.[8] In our study we observed continuous decrease of a over entire molar mass range, i.e., from the molar mass of about 10^4 g/mol, and the same [η] versus M dependence obtained by on-line and capillary viscometers. Different shearing forces can be expected in viscometers of different design (Ubbelohde versus on-line viscometer). It is also worth mentioning that the measurements in the two types of viscometer are typically carried out at significantly different concentrations. In our particular case, the maximum concentration of the molecules eluted from SEC columns was about 10^{-5} g/mL, i.e., an order of magnitude lower than the minimum concentrations used in the measurements with Ubbelohde viscometer. Consequently, one would expect different onset of the non-Newtonian behavior in the two different viscometers, but the plots in Figures 4
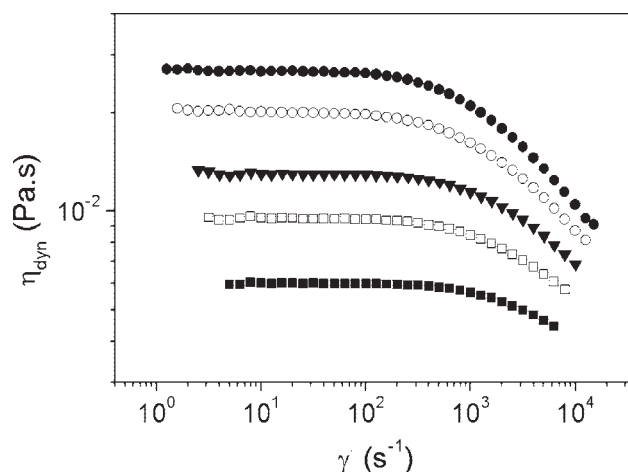

Figure 8 Flow curves of HA solutions ($M_w = 7 \times 10^5$ g/mol) at different concentrations in 0.1M sodium phosphate buffer. HA concentrations: ($\bullet$) 3.17×10^{-3} g/mL, ($\bigcirc$) 2.41×10^{-3} g/mL, ($\blacktriangledown$) 1.90×10^{-3} g/mL, ($\square$) 1.59×10^{-3} g/mL, and ($\blacksquare$) 0.96×10^{-3} g/mL.
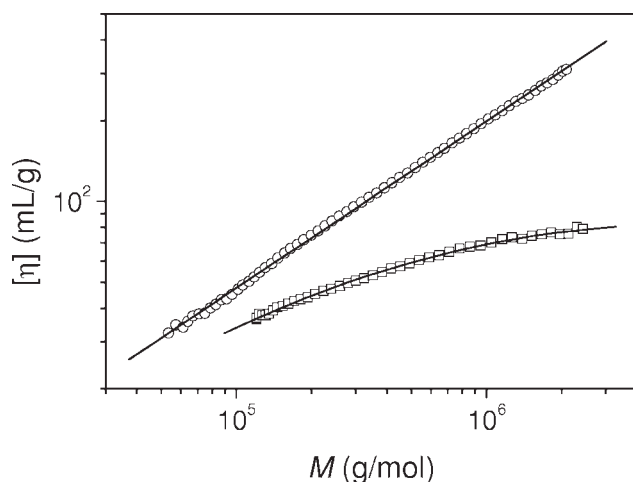
Figure 9 Mark-Houwink plots of pullulan (○) and dextran (□) obtained by SEC-MALS-VIS measurements of polydisperse pullulan (Polymer Laboratories, nominal $M_w = 3 \times 10^5$ g/mol) and polydisperse dextran (Fluka, nominal $M_w = 5 \times 10^5$ g/mol). The Mark-Houwink equation for pullulan: $[\eta] = 0.037 \times M^{0.622}$ (50 mM Na_2SO_4, 25°C), $r = 0.999$. SEC conditions as in case of HA, sample concentrations 0.5% w/v and 0.25% w/v for pullulan and dextran, respectively.

and 5 have very similar profile and the change of a with molar mass is almost identical.

An example of flow curves of HA solutions of different concentrations is depicted in Figure 8. In Ubbelohde viscometer with the capillary diameter of 0.636 mm the $\dot{\gamma}_{max}$ calculated according to eq. (3) is about 750 s^{-1} at the concentration of 0.7×10^{-3} g/mL (the highest concentration used for the Ubbelohde measurements for this sample). It can be seen from Figure 8 that non-Newtonian effect for solution with the concentration of about 1 mg/mL is negligible up to $\dot{\gamma}$ of about 800 s^{-1} and markedly lower effect can be expected for lower concentrations which were used for the Ubbelohde measurements. Actually, the explanation of the decrease of the intrinsic viscosity as a result of non-Newtonian behavior is highly questionable. The intrinsic viscosity is a measure of the hydrodynamic volume of a polymer molecule in a dilute solution, not the solution viscosity itself. The intrinsic viscosity may increase while the solution viscosity decreases as in case of the increase of intrinsic viscosity with temperature. The intrinsic viscosity is determined from the y-axis intercept of the concentration dependence of reduced viscosity and the non-Newtonian behavior, being more prominent at higher concentrations, would in fact result in the decrease of the slope of the concentration dependence of reduced viscosity and overestimation of the intrinsic viscosity.

The decrease of a with increasing molar mass is typical for branched polymers, while the a of linear polymers is constant over a broad range of molar masses. The illustration of this fact is shown in Fig-

ure 9 that contrasts the Mark-Houwink plots of linear polysaccharide pullulan with branched polysaccharide dextran. The Mark-Houwink plot of pullulan is perfectly linear while that of dextran is curved resembling the plot of HA. Despite similar chemical composition of both polysaccharides, the intrinsic viscosity of branched dextran is lower than that of linear pullulan with the same molar mass. In randomly branched polymers, the difference between the intrinsic viscosities of branched and linear molecules increases toward high molar masses as the probability that a macromolecule contains a branch unit increases with increasing molar mass. HA is generally believed to be a linear biopolymer as was determined by Weissmann and Meyer already in 1954.[1] The linear structure was assumed on the basis of chemical evidence, but the authors admitted the presence of a few branches in a HA molecule. However, a few branch points in a polymer chain consisting of several thousands structural units can easily elude detection. During fermentation by HA synthases no branches in the HA chain should be formed according to Weigel.[20] Nevertheless, quite harsh cleaning procedures follow the fermentation step, during which various side reactions may occur. It is worth mentioning that solely a single branch unit in a polymer chain results in measurable decrease of molecular dimensions.[21]

Useful information about the conformation of polymer molecules can be obtained from so-called conformation plot, i.e., log–log relation between the root mean square (RMS) radius and molar mass. The conformation plots for two samples of HA are depicted in Figure 10. Both plots are linear with the slopes of 0.49 and 0.50. It is generally accepted that the slopes of conformation plots for linear polymers in thermodynamically solvents are ∼ 0.58, and that the lower slopes indicate branching.[22,23] Therefore,
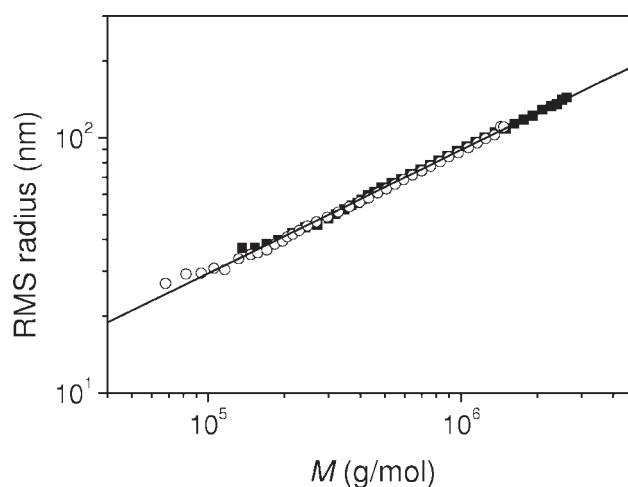

Figure 10 Conformation plots of two HA samples (Berry formalisms used for data processing).

the plots in Figure 10 may provide additional evidence of branching. As the intrinsic viscosity and RMS radius are mutually related, one would expect the conformation plots to be curved in a similar manner as the Mark-Houwink plots. The conformation plots having a constant slope and corresponding Mark-Houwink plots with the slope decreasing as a function of molar mass were reported by Mendichi et al.[3] who explained this behavior by the "change of the partial draining nature of charged chains with their length." Another possible explanation of the discrepancy of the shape of the Mark-Houwink plots and the conformation plots is limited resolution of SEC. The determination of Mark-Houwink plot and conformation plot by SEC-MALS-VIS assumes extremely narrow fractions at each elution volume slice. If the SEC separation is less efficient and the polydispersity of elution volume slices is not negligible, the z-average RMS radii or the weight-average intrinsic viscosities are plotted against the weight-average molar masses. In SEC the resolution decreases with increasing molar mass and such the polydispersity is likely to increase toward high molar masses. Another factor contributing to the increased polydispersity at high values of molar mass may be presence of fractions exceeding the exclusion limit of SEC columns. Because of the increased polydispersity, the RMS radius and molar mass values determined by the MALS detector are higher than they would be for strictly monodisperse fractions. As the z-average RMS radius is more sensitive to the polydispersity than the weight-average molar mass, the expected downward curvature of the conformation plot may be eliminated as a result of the overestimation of the RMS radius. In contrast to the conformation plot, the Mark-Houwink plot relates the same moments of the intrinsic viscosity and molar mass and such the effect of polydispersity is significantly lower. In addition, one has to take into account that the conformation plot is generally less inclinable to the curvature. According to the Flory-Fox equation, the relation between the Mark-Houwink exponent a and the slope of the conformation plot b is $b = (1 + a)/3$. The a values are in the range of 0 to about 1 for compact spheres and expanded coils, respectively; and such b can correspondingly vary solely within the range of 0.33 to 0.67, which makes the conformation plot always less curved than the Mark-Houwink plot.

CONCLUSION

It can be concluded that previously reported explanations of the decreases of Mark-Houwink exponent a may be questioned in the view of presented results. As the Mark-Howink plots obtained by different types of experiments are similar and have pattern typical for branched polymers, we suggest that HA chains are branched and not entirely linear as generally assumed. The conclusion based on the Mark-Houwink plots is supported by conformation plots. The branching may occur as a result of side reactions during the manufacturing procedure. It should be emphasized that molar mass dependence of the Mark-Houwink parameters of HA makes the determination of molar mass by classical capillary viscometer highly inaccurate. The fact that HA most likely contains branched macromolecules certainly does not affect its biological applications. It only brings deeper insight into the molecular structure of this interesting and important polymer and may contribute to better understanding the properties of aqueous HA solutions.

References

1. Weissmann, B.; Meyer, K. J Am Chem Soc 1954, 76, 1753.
2. Lapcik, L.; Lapcik, L.; De Smedt, S.; Demeester, J.; Chabrecek, P. Chem Rev 1998, 98, 2663.
3. Mendichi, R.; Soltes, L.; Schieroni, A. G. Biomacromolecules 2003, 4, 1805.
4. Waters, J.; Leiske, D. LCGC North Am 2005, 23, 302.
5. Hokputsa, S.; Jumel, K.; Alexander, C.; Harding, S. E. Carbohydr Polym 2003, 52, 111.
6. Bothner, H.; Waaler, T.; Wik, O. Int J Biol Macromol 1988, 10, 287.
7. Shimada, E.; Matsumura, G. J Biochem 1975, 78, 513.
8. Gura, E.; Hückel, M.; Müller, P. J. Polym Degrad Stab 1998, 59, 297.
9. Bezakova, Z.; Hermannova, M.; Drimalova, E.; Malovikova, A.; Ebringerova, A.; Velebny, V. Carbohydr Polym 2008, 73, 640.
10. Kulicke, W. M.; Clasen, C. Viscosimetry of Polymers and Polyelectrolytes; Springer-Verlag: Berlin Heidelberg, 2004; p 43.
11. Vold, I. M. N.; Kristiansen, K. A.; Christensen, B. E. Biomacromolecules 2006, 7, 2136.
12. Laurent, T. C.; Ryan, M.; Pietruszkiewicz, A. Biochim Biophys Acta 1960, 42, 476.
13. Armstrong, D. C.; Johns, M. R. Biotechnol Tech 1995, 9, 491.
14. Nimrod, A.; Greenman, B.; Kanner, D.; Landsberg, M.; Beck, Y. U.S. Pat. 4,780,414 (1988).
15. Yanaki, T.; Yamaguchi, M. Chem Pharm Bull 1994, 42, 1651.
16. Terbojevich, M.; Cosani, A.; Palumbo, M.; Pregnolato, F. Carbohydr Res 1986, 149, 363.
17. Li, M.; Rosenfeld, L.; Vilar, R. E.; Cowman, M. K. Arch Biochem Biophys 1997, 341, 245.
18. Soltes, L.; Mendichi, R.; Lath, D.; Mach, M.; Bakos, D. Biomed Chromatogr 2002, 16, 459.
19. Ghosh, S.; Khobal, I.; Zanette, D.; Reed, W. F. Macromolecules 1993, 26, 4684.
20. Weigel, P. H. IUBMB Life 2002, 54, 201.
21. Zimm, B. H.; Stockmayer, W. H. J Chem Phys 1949, 17, 1301.
22. Podzimek, S.; Vlcek, T. J Appl Polym Sci 2001, 82, 454.
23. Wyatt, P. J. Anal Chim Acta 1993, 272, 1.